Supplementary figure legends

Figure S1

A) UP-regulation of H3K9me3 is always detected independently from the normalization technique. Outcome of different normalization techniques on the amounts of up- and down- regulated regions. X-axis, p-values, y-axis, total length of up- and down-regulated regions (in base pairs). In the first option, the library size (that is, amount of sequenced reads) in the mappable genome (that is, uniquely mapped reads) was used to calculate normalization factors with a geometric mean. Geometric mean is less sensitive than arithmetic mean to outliers in skewed distributions, which are typical in ChIP-seq. Second solution is the same as first but with arithmetic mean. In the last solution, which was used in all the analysis of this manuscript, only the reads within the peaks are used to calculate normalization factor, with geometric mean. Notably, independently from the solution used, a large amount of up-regulated regions is found at $p<0.001$ and even at considerably more stringent p-values. Vice versa, total length of down-regulated regions is much lower already at $p<0.001$ and, most importantly, quickly disappears when increasing the stringency.

B) Reproducibility of H3K9me3 UP-regulation in the H3K9me3-repressed stretches longer than 25kb. Heatmap, each line represents a stretch of facultative heterochromatin marked by H3K9me3 (we found 617 of such blocks via peak calling). Stretches are sorted in chromosomal order, by start site. The color indicates the average up-regulation found in various developmental stages of the hippocampus or adult brain areas. In each condition, at least two biological replicas (littermates) were used (total of 36 samples in 8 conditions). *Ehmt1*$^{+/-}$ has consistently higher methylation levels in many H3K9me3 stretches, showing very high reproducibility. Genome-wide, 77% of the H3K9me3 blocks longer than 50kb presents significantly ($p<0.001$) increased methylation in *Ehmt1*$^{+/-}$ samples. Vice versa, *Ehmt2*$^{+/-}$ shows overall weaker up-regulation.

C) Reproducibility of H3K9me3 UP-regulation. Different developmental stages and brain areas were tested for an increase (left) or a decrease (right) of H3K9me3 in *Ehmt1*$^{+/-}$ mice. The central cores correspond to regions which are up-regulated with Zscore>1 ($p < 0.15$) in each developmental stage and brain area (final probability considering independent experiments $p<2.5e-6$). Notably, while a highly conserved and large (>50Megabases) core of regions consistently up-regulated in multiple conditions was found, intersection of down-regulated regions is almost empty. Therefore, down-regulated regions are not as reproducible as the up-regulated ones.

D) Analysis of DNA methylation data, example. Methylation and coverage were quantified in the promoters (Transcription Start Site +/- 2kb) genome-wide. Sequencing noise (dispersion on the y-axis) is inversely proportional to the sequencing depth, i.e. coverage (x-axis). In other terms, regions with lower coverage display higher variability across samples which eventually results in larges fold changes when comparing different samples/conditions. Fitting of the technical dispersion as a function of the coverage was calculated with a moving average of the standard deviation. Points (promoters) exceeding the fitting line (in this example set at $p<0.0001$) are considered significantly changed in methylation.

Figure S2

A) H3K9me3 UP-regulation is present in multiple brain areas. Wild type and *Ehmt1*$^{+/-}$ H3K9me3 samples from frontal cortex, olfactory bulb and cerebellum (20 samples, littermates) were analyzed. As a first step, we selected all the regions displaying significant ($p<0.001$, sliding-window/merging approach, see methods) deregulations in H3K9me3 levels in at least one brain area. Subsequently, regions were clustered (kmeans/trajectory clustering with squared euclidean distance, see methods) according to their normalized (with respect to wild type hippocampus) expression levels. As a result we isolated 6 different clusters (C1-C6) **Left)** Pie chart, slices are proportional to the size (base pairs) of the clusters. **Right)** Centroids (mean, 25th and 75th percentiles) of the clusters. In the largest cluster C1, physiological (wild type) H3K9me3 is stable across brain areas and, at the same time, displays a marked increase of intensity in each *Ehmt1*$^{+/-}$ counterpart. In C2 and C3, physiological H3K9me3 is higher in frontal cortex (compare blue bars) but again all the areas present increased (stronger in C3, weaker in C2) H3K9me3 in *Ehmt1*$^{+/-}$ mice. Aside from olfactory receptors and similar genes, also several (17) protocadherins are included in the regions of C2 and C3. Only in a minor number of loci (C4-C6) UP-regulation of H3K9me3 is not present with the same strength in all brain areas.

B) Example. H3K9me3 (average +/- SEM) repressing clustered olfactory receptors genes in the qC1 cytoband of chr14, 380 kb wide. This H3K9me3 block is constituted by regions of C1, i.e. regions with i) stable levels of H3K9me3 across wild type brain areas and i) UP-regulation of H3K9me3 in each brain area.

Figure S3

A) H3K9me3 UP-regulation is found already at P1 Wild type and *Ehmt1*$^{+/-}$ H3K9me3 samples from P1, P7, P15 and P30 stages (20 samples, littermates) were analyzed. As a first step, we selected all the regions displaying significant ($p<0.001$, sliding-window/merging approach, see methods) deregulations in H3K9me3 levels in at least one stage. Subsequently, regions were clustered (kmeans/trajectory clustering

with squared euclidean distance, see methods) according to their normalized (with respect to wild type hippocampus) expression levels. As a result we found only one main clusters in which H3K9me3 levels of mutant hippocampus are higher than wild types in each developmental stage, starting already at P1. A moderate developmental increase of H3K9me3 is found in wild-type (possibly because of an increase of differentiated mature cells which display higher H3K9me3 [1]) but especially mutant hippocampi.

B) Example. H3K9me3 (average +/- SEM) repressing clustered *Clec* genes in the qF1 cytoband of chr6, 300 kb wide. Dispersion (SEM) is lower at P30 stage because it has more (4) biological replicas than other stages (2).

C) None of the H3K9 (de)methyltransferases or (de)acetyltransferases results deregulated. Heatmap of the p-values calculated by DEseq2 by comparing tag counts in wild type and *Ehmt1*$^{+/-}$ littermates (H3K36me3 in gene bodies, RNAseq in exons, other marks in the promoters). *AU041133* is the gene with the statistically strongest epigenetic repression genome-wide and is here presented as an example of deregulation. Unlike AU041133, none of the other genes shows multiple, consistent deregulations in epigenetic makeup and expression.

Figure S4

A) Calculation of Deregulation score (D_{score}). In order to exploit the cross-talking/redundancy of histone marks and calculate one single index representing the severity/reliability of a deregulation, we integrated the data of RNA-seq and histone marks into an index called D_{score}. Here, the method is illustrated using as an example *Tdo2*, the gene with the strongest UP-regulation (D_{score} = +14,9) in *Ehmt1*$^{+/-}$ hippocampus. As a first step, each element is analyzed individually in order to calculate its p-value. For RNAseq we compare the tags mapped in the exons. For H3K36me3 we compare the tags mapped in the gene bodies. For H3K4me3 and H3K27ac, peaks are called and linked to promoters. Tags in peaks were then compared. For the remaining marks (H3K27me3, H3K9me2, H3K9me3, H3K4me1) we compared the tags mapped in the promoters (TSS+/-2kb). For DNAme we compare the methylation of the CpG island near the promoter. If no CpG island is detected, we compare the methylation of the promoter (TSS+/-2kb). All the p-values are calculated with DEseq2 apart from DNAme, for which a different approach is used (Fig.S1D). P-values are transformed to Zscores and hence gain a sign (+ for UP-regulation, - for DOWN-regulation). Zscores of repressive marks (H3K27me3, H3K9me2/3, DNAme) are then inverted. In this way Zscores with the same sign indicate concordance among epigenetic marks, whereas Zscores with the opposite signs indicate not

concordant changes (as for instance it could be increase of H3K4me3 and decrease of RNAseq). Subsequently, Zscores are sorted from the highest to the lowest. For *Tdo2*, the highest is the Zscore of H3K4me3 (5.8, originated from p<3e-9) whereas the lowest is -0.125 (H3K27me3). At this point, we sum the three highest Zscores to the three lowest Zscores to obtain the D_{score}, which in the case of *Tdo2* results to be 14,8. The main advantage of the D_{score} is that it rewards concordant changes in epigenetic marks whilst penalizing not concordant ones (in the case of *Tdo2*, only H3K27me3 gives a minor negative contribution to the score as considering the overall change in epigenetic makeup it was expected to decrease). Moreover, this approach allows genes in which only a subset of marks is changed to get high D_{scores}, as only three marks (the TOP three from UP-regulation, or the lowest three for DOWN-regulation) become the main drivers of the final score. Last aspect essentially takes into account that histone marks not necessarily always change altogether.

Eventually, we decided to drop the Zscore of DNAme in the calculation of D_{score}. In fact, DNAme appears highly redundant, as all the genes presenting significant changes in RNA-seq and histone marks always present concordant changes of DNAme (Table S1, GEO). In this sense DNAme adds nothing to what it can be already computed. On the other hand, there are also many promoters (CpG islands) in which only a change in DNA methylation is found without corresponding changes in any histone marks nor RNAseq. We do not consider these cases as reliable deregulations and we therefore excluded the DNAme from the D_{score} calculation. However, DNA methylation is considered in all the analyses (example, boxplots shown in **-C-**) following the D_{score} calculation. The threshold for calling significant deregulation was set to D_{score}>6 (UP) and D_{score}<-6 (DOWN). Additionally, we required the deregulated genes to present a significant (p<0.05) change in RNAseq or at least one of the activating marks (H3K4me3, H3K26me3, H4k27ac, H3K4me1). This is because we want to focus on the actively expressed genes, discarding those (numerous) silenced olfactory receptors and similar families which present highly significant increase of H3K9me2 and H3K9me3 in their promoters but nothing else. As the final result, we found 53 UP-regulated genes and 160 DOWN-regulated genes. The genes whose D_{scores} fall near the main percentiles are shown in the lower plots (only the marks with |Zscore|>1.28, ie p<0.1 are shown). P-values (*p<0.05, **p<0.025, ***p<0.01). Tag counts on the Y-axis are omitted for simplicity. Genes closer to the lowest (less significant) percentile, *Efna5* and *Kcnrg*, already show clear changes in expression levels and histone marks when comparing wild type to *Ehmt1*$^{+/-}$ mice, indicating that the threshold of 6 efficaciously isolates significant deregulations. Increasing D_{scores} correlate with involvement of a larger number of marks and/or severity of deregulations, as in the cases of *Samd9l* and *Fam26e*.

B) Clusters of deregulated genes. Boxplot, mean +/- SEM and 99% confidence interval for RNAseq, histone marks and DNA methylation. **Left)** DOWN-regulated genes, cluster 2. This cluster collects genes presenting a very mild increase of repressive marks, including also H3K27me3, concomitantly to a decrease in expression and active marks. Genes in this cluster are enriched in epithelium development ($p<7.3e-3$) and include important regulators of brain development such as *Bmp2* and *Bmp3,* which is show in **(A)** with D_{score}=-7.6. The main differences with the cluster 1, shown in Fig.3A, are i) change of H3K27me3 ii) overall milder fold changes. **Center)** DOWN-regulated genes, cluster 3. This cluster collects genes with very high increase of H3K9me3 and, to a minor extent, Hk39me2, and variable decrease of expression (RNAseq), H3K36me3 and H3K4me1. This cluster is rich in olfactory receptors, which are subjected to a strong increase of H3K9me3 but, being very poorly expressed (ie, very few tag in RNAseq and active marks), show noisy variability in the reduction of RNAseq and active marks. **Right)** UP-regulated genes. A mild decrease of H3K9me2 correlates with a pronounced increase of expression and active histone marks (especially H3K4me3). The remaining gens (13) which do not fit any of the clusters are not shown.

Figure S5

A) H3K4me3 is decreased in the promoters of protocadherins in multiple brain areas. Upper) Heatmap, blue color, indicating significant decrease of H3K4me3, is present throughout most protocadherins and brain areas. **Lower)** Boxplot. The average fold change of these 26 protocadherins is represented. Overall, protocadherins are consistently DOWN-regulated in hippocampus, frontal cortex, olfactory bulb and cerebellum. Stronger repression is found in cerebellum.

B) *Ehmt1*$^{+/-}$ limited and specific interplay with postnatal development. Genes changing expression (H3K4me3 and RNAseq) during wild type postnatal development of hippocampus amount to 5549 (see methods). Genes deregulated in *Ehmt1*$^{+/-}$ samples (H3K4me3 and RNAseq) in the course of postnatal development amount to 255 (see methods). Intersection among the two gene sets amounts to 109 genes, meaning that 109/255 of the *Ehmt1*$^{+/-}$ deregulated genes are also meant to change expression in the course of physiological postnatal development, whereas 146/255 constant expression level during postnatal stages.

C-G) Clusters and examples of *Ehmt1*$^{+/-}$ deregulations during development. Boxplot, mean +/- SEM and 99% confidence interval for RNAseq and H3K4me3. Kruskal-wallis is used to test the hypothesis of different means in RNA-seq and H3K4me3 of log2(*Ehmt1*$^{+/-}$/wt) in the different stages. Examples of

Ehmt1$^{+/-}$ deregulated genes are represented in the bar charts. Y-axis, number of tags, normalized to P1 level, mean +/- SEM. DEseq2 p-values (*p<0.05, **p<0.025, ***p<0.01). The 5549 Developmentally regulated genes during postnatal development were segregated in four different expression patterns: UP, DN, STABLE, OTHERS (see methods). Genes with increased/decreased expression in adult stage belong to the UP/DOWN group. STABLE genes do not change expression. OTHERS change expression, but with transient variations which are neither UP nor DN**.** Genes of clusters C1 to C5 were further segregated according to their developmental expression pattern (stacked histogram to the right of each boxplot). In each cluster the majority of genes is stably expressed during postnatal development. **(C)** In C2, genes UP-regulated in *Ehmt1*$^{+/-}$ appear slightly (p=0.034, RNAseq) more UP-regulated in later stages (P15 and P30). Instead, UP-regulation of H3K4me3 is stable during development (p>0.01). *Scn7a*, a subunit of sodium voltage-gated channels, as an example. It belongs to the subgroup of STABLE genes. **(D)** In C3, genes DOWN-regulated in *Ehmt1*$^{+/-}$ display an increase of the deregulation at P15 stage (p<6.7e-13, RNAseq data). H3K4me3 displays neglectable and unstable (p<1e-5) DOWN-regulation. Interestingly C3, compared to other clusters, contains a higher proportion of genes UP-regulated during regular (wild type) postnatal development (15/36 UP). As an example, *Ccr5*, a chemokine receptor UP-regulated during postnatal development which displays a peak of abnormal DOWN-regulation at the P15 stage. **(E-F)** The two smaller clusters (C4,C5) collect genes in which RNAseq (C4) or H3K4me3 (C5) becomes progressively UP-regulated during development. *Wdr95* (RNAseq) and *4930447N08Rik* (H3K4me3) reported as examples. RNAseq and H3K4me3 can show, in some cases, weak correlation. Change of transcript expression (C4) does not necessarily require an epigenetic change in the H3K4me3 levels whereas weak RNAseq change concomitant to H3K4me3 change (C5) can be caused for instance by additional changes in the mRNA metabolism, such as a change in the mRNA stability. **(G)** Segregation of cluster 1 (Fig.3D) genes according to their developmental expression pattern.

Figure S6

A) Table of the epigenetic deregulations for the clustered protocadherins in *Ehmt1*$^{+/-}$ and *Ehmt2*$^{+/-}$ P30 hippocampi. A positive(negative) Z-score is colored in red(blue) and indicates up(down)-regulation in mutants compared to wt. For different ChIP-seq, different regions were used to compare wild-types against mutants: “prom” indicates promoters, “bodies” indicates gene bodies and “peaks” indicates the peaks found with peak calling (see methods for details). The significantly down-regulated protocadherins with D-score<-6 are marked by orange and gray colors: only two protocadherins, namely *Pcdha12* and *Pcdhb1*, are down-regulated in *Ehmt2*$^{+/-}$. Interestingly, in *Ehmt1*$^{+/-}$ hippocampus, down-regulation seems

to be follow a gradient both in the *beta* and *gamma* clusters. In *beta* cluster, *Pcdhb1/2* and *Pcdhb12-19* feature the strongest down-regulation, as shown by the Z-scores of RNA-seq, H3K4me3 ChIP-seq and partially also H3K27ac. In the *gamma* cluster, strongest down-regulation is found in the initial protocadherins, *Pcdhga1-4* and *Pcdhgb1-4,* as shown by the down-regulation of H3K36me3 and partially also H3K4me3 and H3K27ac. Please note that in the current table for the gamma cluster the expression comparison (RNA-seq) was performed at the level of the individual alternative isoforms by considering only the reads falling in the alternately spliced exon and discarding the reads in the common, constitutive exons. Here, the ability of RNA-seq to detect deregulated isoforms is limited by the single-end sequencing and therefore ChIP-seq data is more reliable and sensitive.

B) Q-PCR validation of the gradient down-regulation in the *beta* cluster. Comparison was performed by measuring the recovery of the H3K4me3 ChIP samples (three biological replicates). Recovery is always lower in *Ehmt1*$^{+/-}$ samples compared to wild types, validating down-regulation of H3K4me3 in *Pcdhb5*, *14*, *15* and *22*. Furthermore, down-regulation is stronger in *Pcdhb15* and *Pcdhb14,* validating the result found by the genome-wide analysis of Fig.4H.

Figure S7

A) Neurological evaluation of *Ehmt1*$^{+/-}$ and *Ehmt2*$^{+/-}$ mutants for general health, motor abilities or pain sensitivity. **B)** Locomotor activity and rears in the actimetric cages during the light and dark phases. **C, D)** Acoustic startle response and prepulse inhibition. **E)** Social preference (for a congener vs an object) and **F)** social memory (for a novel vs familiar congener) were not affected in *Ehmt1*$^{+/-}$ or *Ehmt2*$^{+/-}$ mutants. **G)** The number of arm entries in the Ymaze and **H)** in the elevated plus maze.

Between groups comparisons were made using one factor or repeated measures ANOVA. Student-Newman-Keuls post hoc was used to compare performance between two groups. *p<0.05, ** p<0.01 vs WT. Paired t-test was used to compare sniffing duration between familiar congener and object or between novel and familiar object in the social test, # p<0.05, ###p<0.001 vs object or familiar congener.

Figure S8

A) Characterization of the *Ehmt2*$^{+/-}$ heterozygous mouse. RNA-seq data (3 heterozygous against 3 wild types) shows a -44% decrease in the heterozygous mice. **(B)** Western blot of EHMT2 (Abcam ab185050, 4

heterozygous and 4 wild type mice) shows an average -78% decrease in the protein level (average calculated over 4 biological replicates and two technical replicates of the Western, intensity normalized over the b-Actin).

References

[1] Jia Liu, Laura Magri, Fan Zhang, Nidaa O. Marsh, Stefanie Albrecht, Jimmy L. Huynh, Jasbir Kaur, Tanja Kuhlmann, Weijia Zhang, Paul A. Slesinger, and Patrizia Casaccia. Chromatin landscape defined by repressive histone methylation during oligodendrocyte differentiation. *The Journal of neuroscience : the official journal of the Society for Neuroscience*, 35(1):352–365, Jan 2015.

SUPPLEMENTARY FIGURE 1

A

AMOUNTS OF UP- AND DOWN- REGULATED BASE PAIRS WITH DIFFERENT NORMALIZATION TECHNIQUES AND DIFFERENT TRESHOLDS FOR THE PVALUES

library size, mappable genome, geometric mean

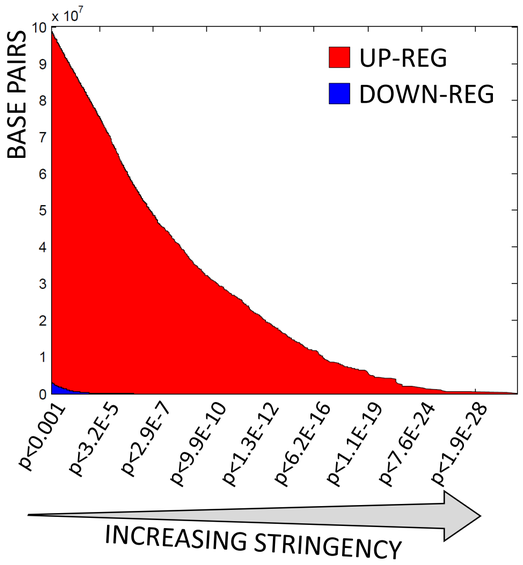

library size, mappable genome, arithmetic mean

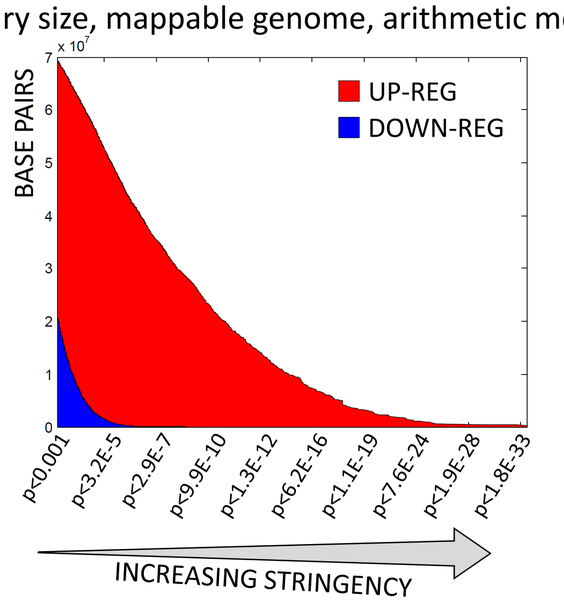

reads in peaks, mappable genome , geometric mean

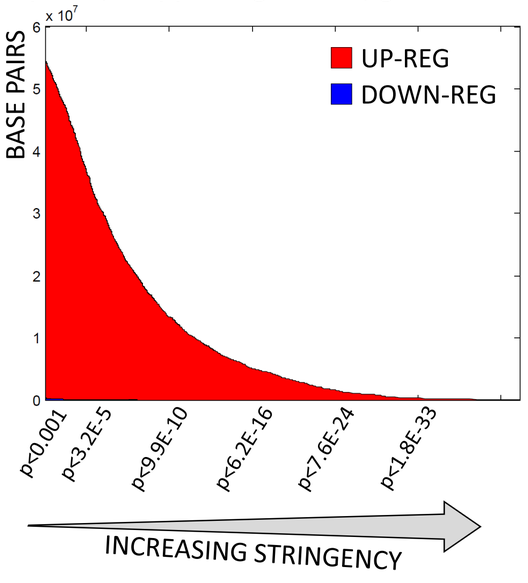

B

H3K9me3 UP-REGULATION IN MULTIPLE BRAIN REGIONS AND DEVELOPMENTAL STAGES (ALL BLOCKS >25Kb)

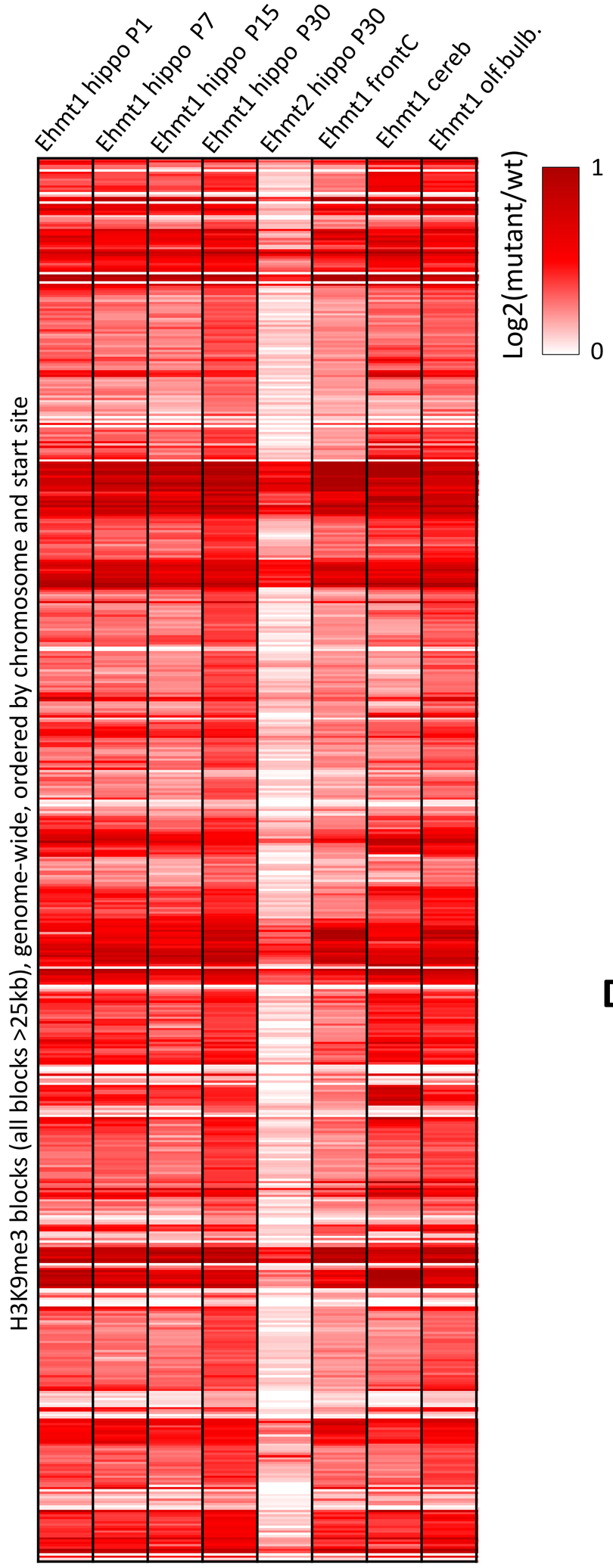

C

REPRODUCIBILITY OF H3K9me3 UP-REGULATED REGIONS

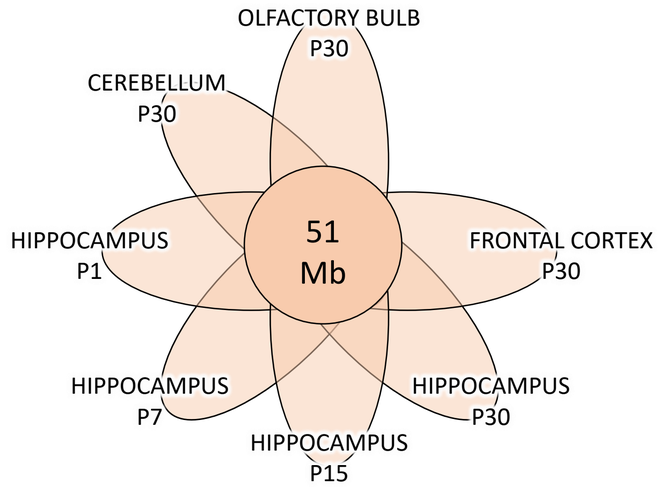

REPRODUCIBILITY OF H3K9me3 DOWN-REGULATED REGIONS

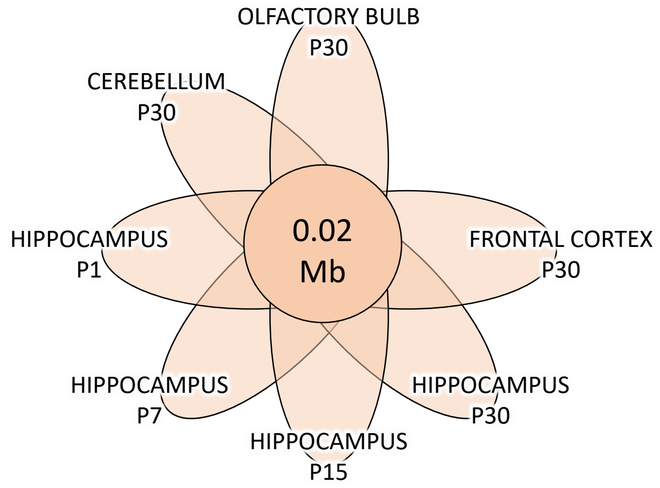

D

DNA METHYLATION ANALYSIS (PROMOTERS)

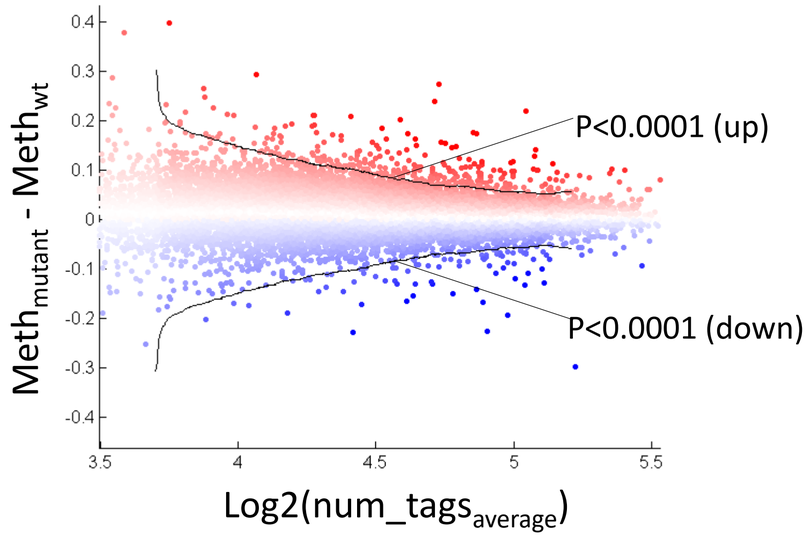

SUPPLEMENTARY FIGURE 2

CLUSTERING OF SIGNIFICANT (*P<0.001*) H3K9me3 UP-REGULATED REGIONS

A

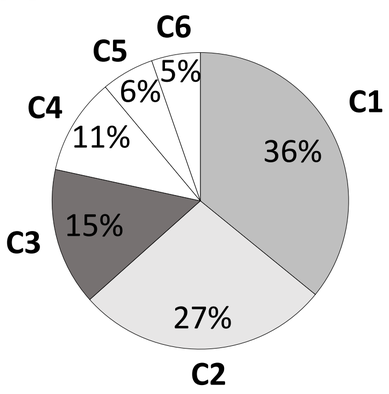

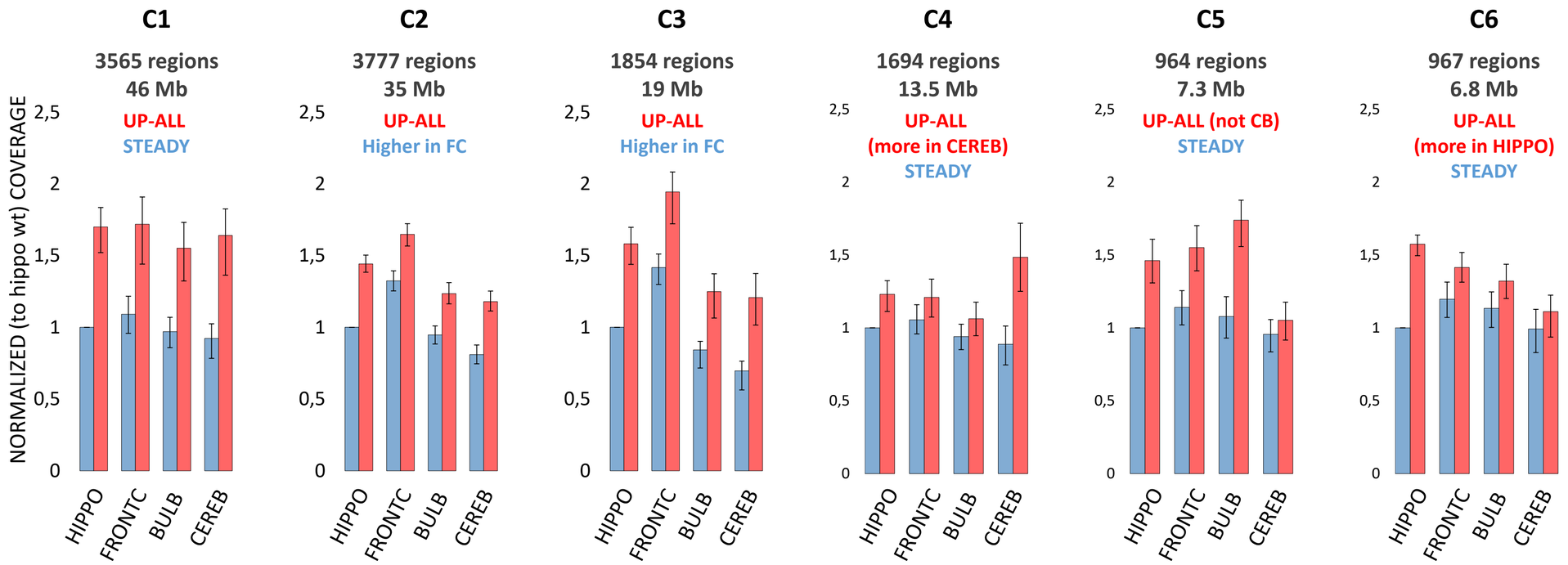

B

Chr14 50`731`501 – 51`111`501 (380kb)

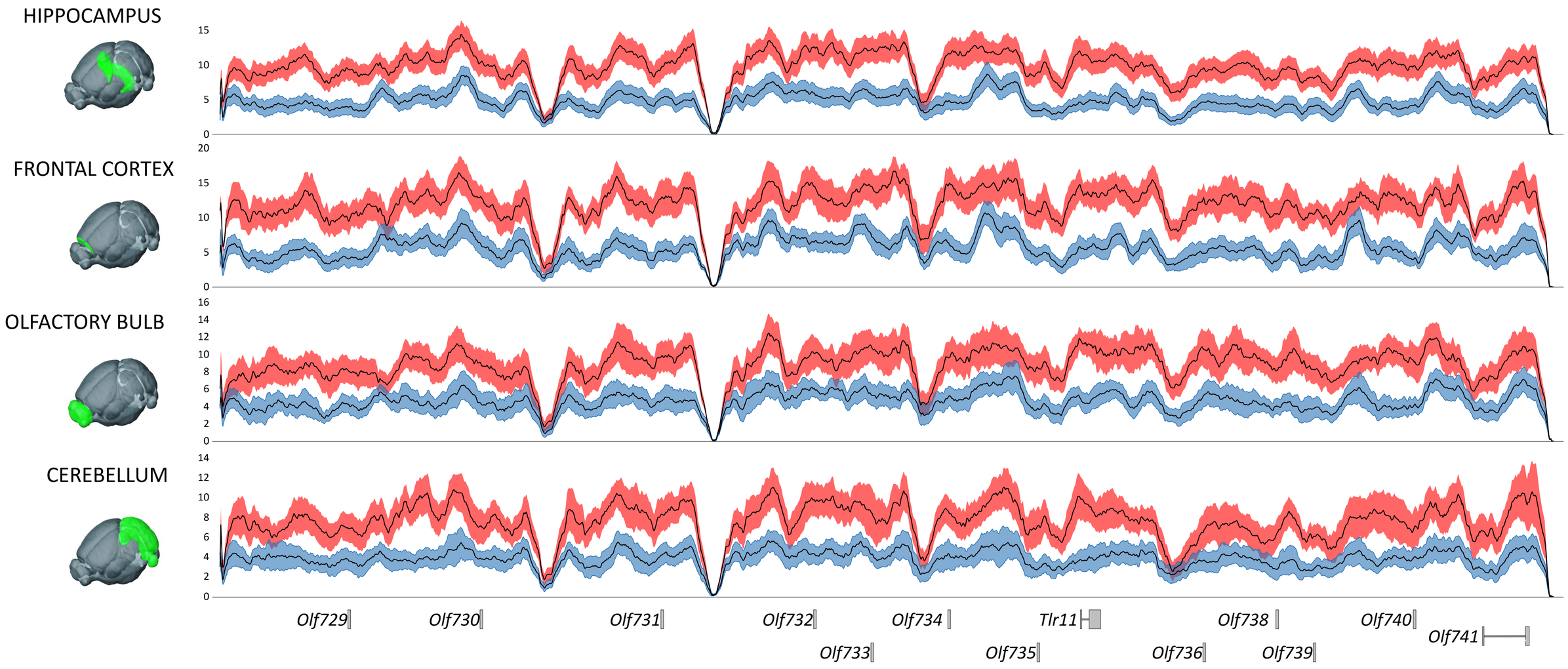

SUPPLEMENTARY FIGURE 3

A

SIGNIFICANT (*P<0.001*) H3K9me3
UP-REGULATED REGIONS

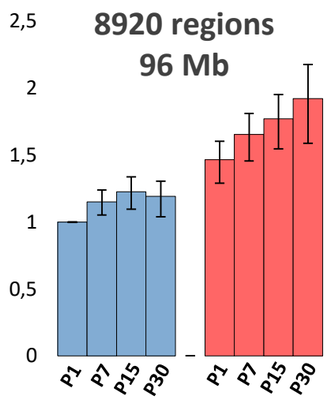

Ehmt1$^{+/-}$ hippocampus

Wild type hippocampus

B

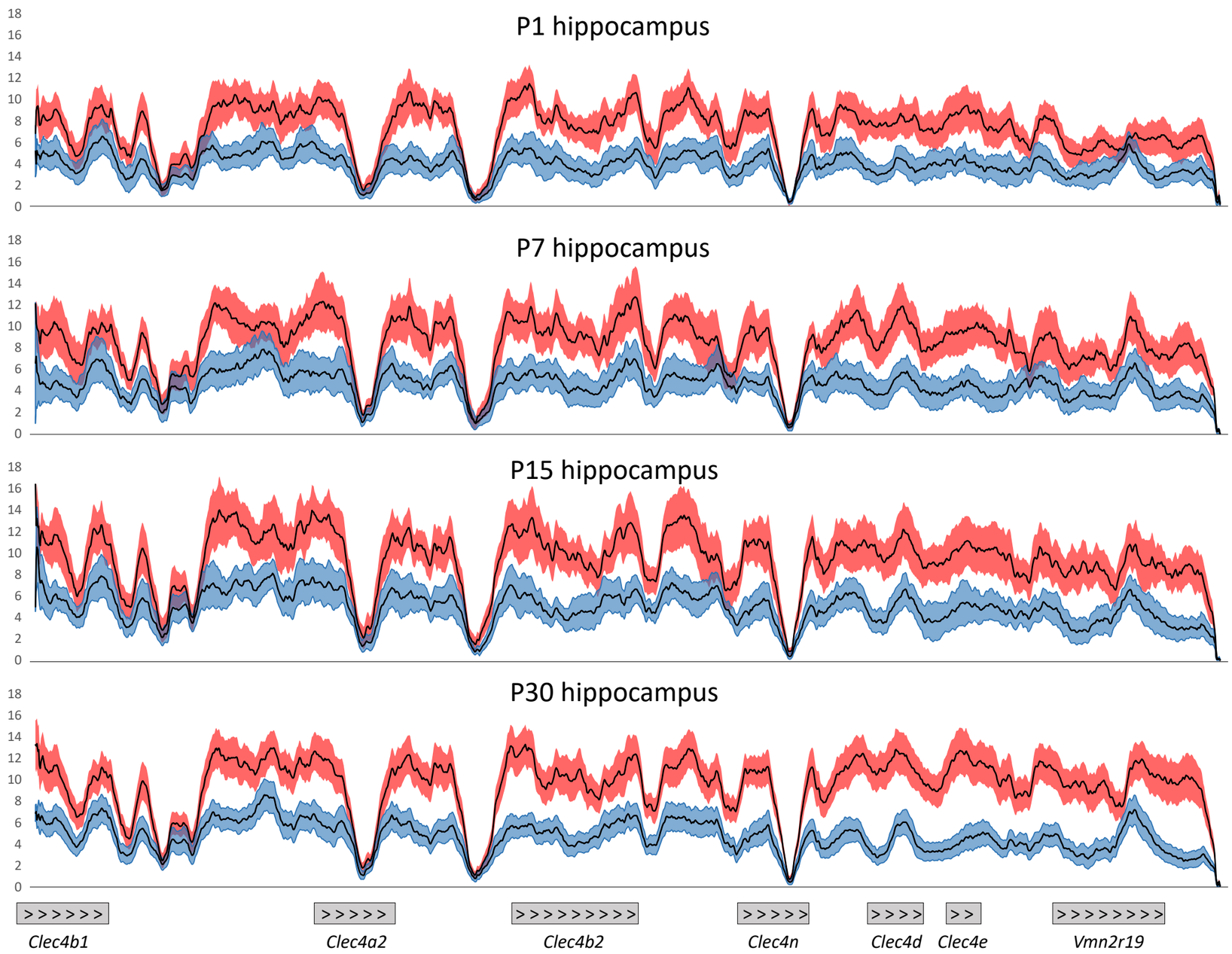

C

SUPPLEMENTARY FIGURE 4

A

Example of calculation of DEREGULATION-SCORE (*Tdo2*)

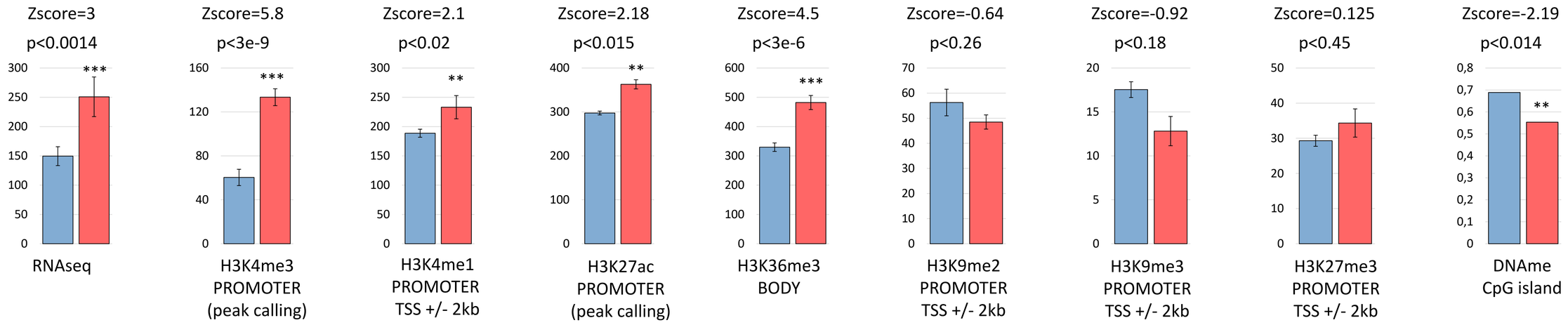

5.8	4.5	3	2.19	2.18	2.1	0.92	0.64	-0.125

highest → lowest

$Tdo2_{D\text{-}score}$ = (5.8+4.5+3) + (0.92+0.64-0.125) = **14.8**

Examples from the 10th ,50th and 90th of Deregulation scores for DOWN-regulated genes

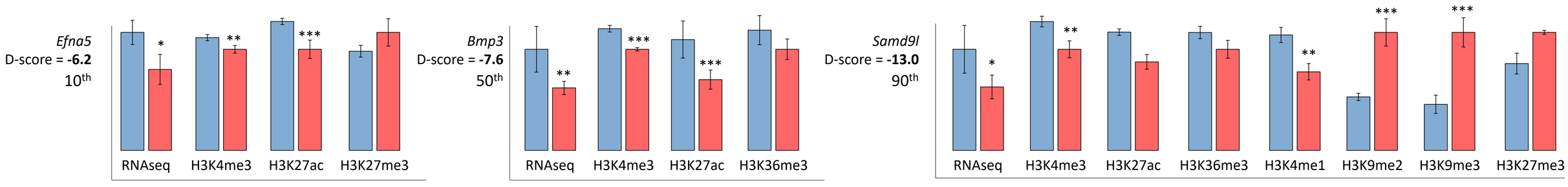

Examples from the 10th ,50th and 90th of Deregulation scores for UP-regulated genes

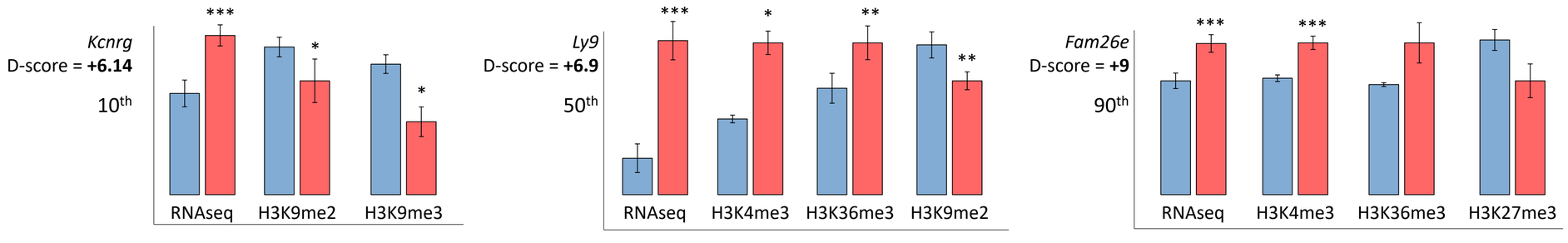

B

SUPPLEMENTARY CLUSTERS OF DEREGULATED GENES

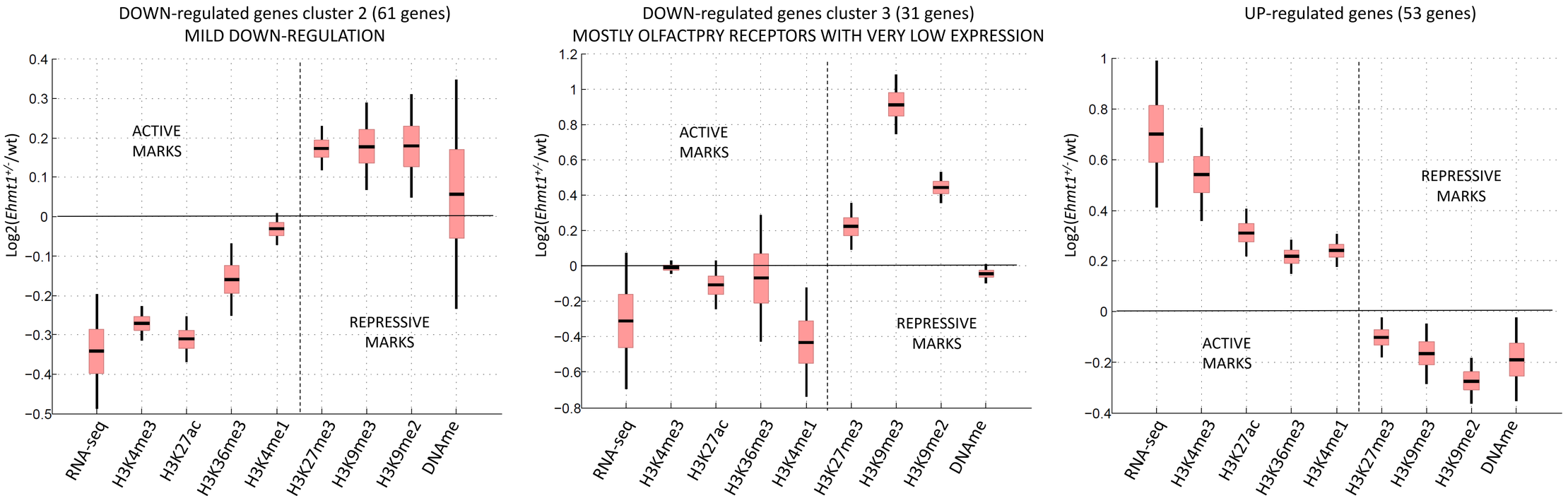

SUPPLEMENTARY FIGURE 5

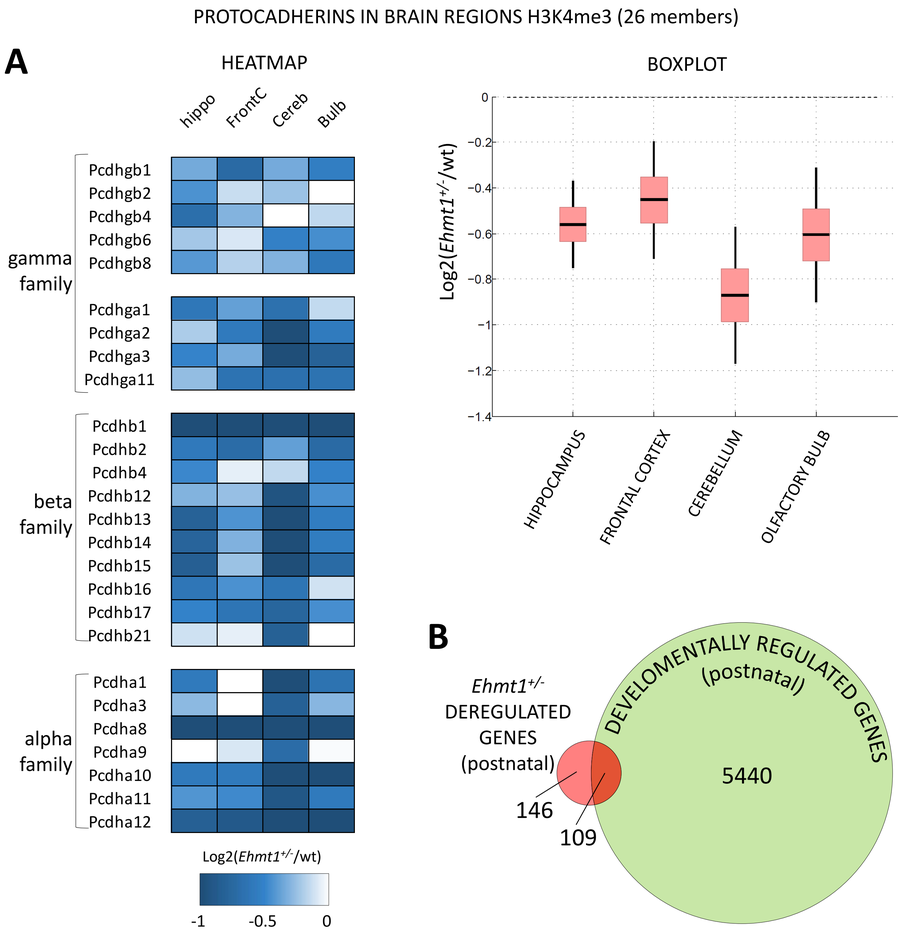

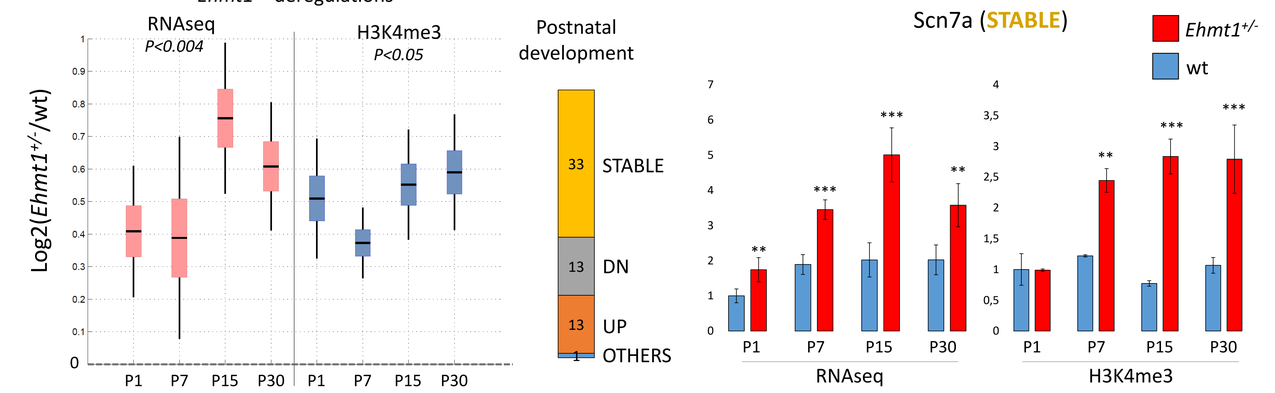

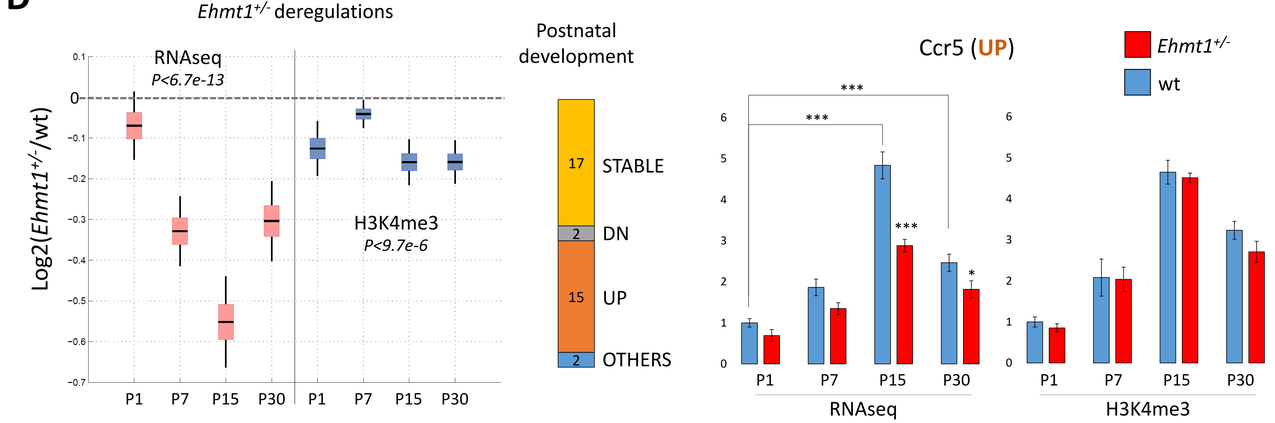

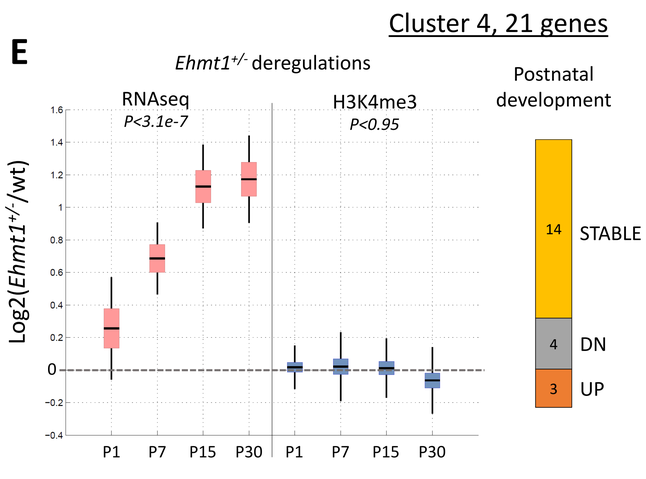

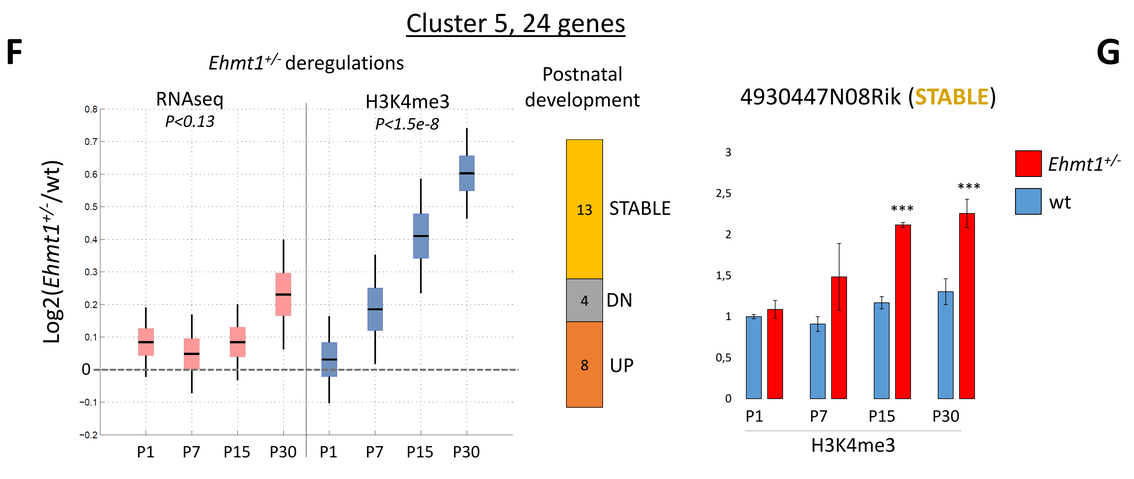

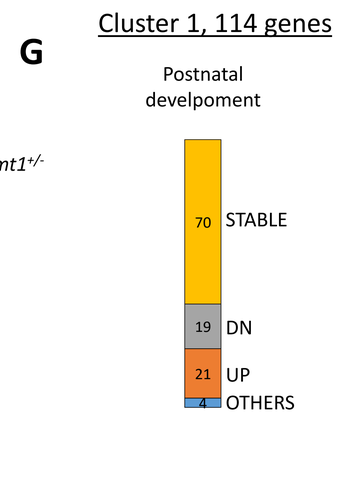

SUPPLEMENTARY FIGURE 6

A Z-SCORES OF EPIGENETIC MARKS AND EXPRESSION DATA IN P30 HIPPOCAMPUS

		Pcdha1	Pcdha2	Pcdha3	Pcdha4	Pcdha5	Pcdha6	Pcdha7	Pcdha7-g	Pcdha8	Pcdha9	Pcdha10	Pcdha11	Pcdha12	Pcdhac1	Pcdhac2	Pcdhb1	Pcdhb2	Pcdhb3	Pcdhb4	Pcdhb5	Pcdhb6	Pcdhb7	Pcdhb8	Pcdhb9	Pcdhb10	Pcdhb11	Pcdhb12	Pcdhb13	Pcdhb14	Pcdhb15	Pcdhb16	Pcdhb17	Pcdhb18	Pcdhb19	Pcdhb20	Pcdhb21	Pcdhb22	Pcdhga1	Pcdhga2	Pcdhga3	Pcdhga4	Pcdhga5	Pcdhga6	Pcdhga7	Pcdhga8	Pcdhga9	Pcdhga10	Pcdhga11	Pcdhga12	Pcdhgb1	Pcdhgb2	Pcdhgb4	Pcdhgb5	Pcdhgb6	Pcdhgb7	Pcdhgb8	Pcdhgc3	Pcdhgc4	Pcdhgc5
EHMT1 samples	RNA-seq ehmt1_P30	0,0	0,0	0,0	0,0	1,0	0,6	0,0	0,0	0,0	0,0	-0,4	0,0	-0,3	0,5	0,0	-0,6	-2,6	-1,7	-0,3	-0,8	0,0	2,5	0,0	0,0	-0,9	-1,6	-2,9	-1,6	-3,4	-5,2	-3,3	-3,9	-0,9	-3,7	-0,3	0,0	-1,0	0,0	-1,1	-3,5	0,2	0,0	0,9	0,0	0,0	0,0	0,0	-0,7	0,0	0,0	-0,3	0,0	-0,6	0,0	-0,3	0,0	0,0	0,0
	ChIP-seq (peaks) ehmt1_P30_H3K27ac	0,0	0,0	0,0	0,0	0,0	0,0	0,0	0,0	-1,1	0,0	-0,6	0,0	-2,3	0,0	0,0	0,0	0,0	0,0	0,0	-1,6	-0,8	0,7	0,0	-1,3	-1,6	0,0	-0,4	-0,8	-2,6	-1,9	-1,2	-0,4	0,0	0,0	-0,2	-0,1	-0,3	-1,2	-0,5	-2,1	0,0	-0,2	0,0	-0,8	0,0	-0,6	-0,9	-1,2	0,0	-1,4	-0,5	-0,6	0,0	-0,2	0,0	-1,5	-0,6	-0,2	-0,2
	ChIP-seq (peaks) ehmt1_P30_H3K4me3	-1,0	2,4	-0,9	-0,1	0,0	1,3	-1,1	-1,1	-2,0	0,0	-1,6	-1,3	-5,7	0,7	0,0	-5,1	-2,3	-0,9	-2,1	0,0	0,0	0,0	0,0	0,0	-1,5	-0,2	-1,1	-2,2	-3,4	-3,2	-2,7	-1,9	-0,3	-1,5	0,0	0,0	0,0	-2,8	-0,4	-2,3	0,0	-1,0	1,2	0,0	0,0	0,0	-0,4	-1,9	0,0	-1,3	-1,7	-2,4	0,0	-0,8	-0,9	-2,8	0,0	-1,1	-1,1
	ChIP-seq (prom) ehmt1_P30_H3K4me1	-0,7	0,0	0,0	-1,1	-0,1	0,2	0,4	0,3	-2,5	0,0	0,0	-0,5	-0,7	0,0	0,3	-2,0	0,0	-0,6	0,0	0,0	0,0	-0,3	0,0	0,0	0,4	-0,7	-1,1	0,0	-0,9	0,0	-2,3	-0,3	0,1	0,0	0,0	0,0	0,0	0,0	-0,3	-1,6	-0,5	-0,3	0,0	0,0	-1,0	-0,7	0,0	0,0	-1,5	0,0	0,0	-0,7	0,0	0,0	-0,5	-2,8	0,0	-0,2	0,0
	ChIP-seq (bodies) ehmt1_P30_H3K36me3	-0,3	-0,1	0,0	-0,3	-0,2	-0,3	-0,3	-2,0	0,0	0,0	0,0	0,0	0,0	0,0	0,0	0,0	-0,9	0,0	-0,5	0,0	-0,5	0,0	0,0	0,0	0,0	-0,1	0,5	0,0	-1,2	0,0	-0,7	-2,0	-0,8	-2,1	0,0	-0,5	-1,0	-3,5	-3,5	-3,4	-3,0	-2,5	-2,0	-1,7	-1,7	-1,4	-1,4	-1,1	-0,6	-3,2	-2,6	-1,7	-1,5	-1,4	-1,3	-0,9	0,0	0,0	0,0
	ChIP-seq (prom) ehmt1_P30_H3K9me3	0,6	2,1	0,1	1,6	2,4	2,6	0,4	0,6	1,9	2,0	3,3	0,9	2,1	0,5	0,0	4,1	3,2	1,9	1,2	1,3	3,1	2,3	0,8	2,0	1,8	1,6	1,7	1,9	0,8	0,3	1,7	1,4	0,6	1,4	0,7	0,7	0,1	0,0	0,0	1,3	1,1	0,9	0,4	1,1	1,6	2,0	1,0	2,0	2,8	1,1	0,8	0,6	1,3	2,1	1,9	2,5	0,0	0,0	0,5
	ChIP-seq (prom) ehmt1_P30_H3K9me2	1,9	3,6	2,7	2,7	4,7	2,4	1,5	1,4	3,3	2,7	3,0	3,0	2,6	0,8	0,0	3,7	3,6	2,0	3,9	3,5	1,3	3,9	1,6	2,4	3,4	3,7	3,4	2,7	2,7	3,7	2,3	2,4	1,9	3,5	3,7	3,3	2,6	3,3	3,2	1,4	3,3	2,0	2,3	2,6	1,1	0,4	2,5	2,8	3,1	3,5	3,4	2,0	2,6	1,7	2,6	2,3	0,0	0,0	0,0
	ChIP-seq (prom) ehmt1_P30_H3K27me3	-0,7	-1,1	-0,4	-0,1	0,0	-0,3	-0,3	-0,8	0,0	0,0	-0,4	0,0	0,0	-1,3	0,0	-1,4	-1,2	0,0	-1,7	-0,1	0,0	0,0	0,0	-0,3	-0,5	-1,4	0,0	-0,6	0,0	-0,8	0,0	-1,8	0,0	0,0	-1,2	0,0	0,0	1,2	1,4	1,7	1,5	0,6	0,0	0,0	0,0	1,0	0,0	0,5	0,0	2,4	1,6	0,5	0,0	0,0	0,9	0,7	-0,8	-0,2	-0,4
EHMT2 samples	RNA-seq ehmt2_P30	-0,1	0,0	0,0	0,0	0,0	0,0	0,0	-0,7	0,0	0,0	0,0	0,0	-0,3	0,0	-0,4	0,0	-0,2	0,0	0,0	-0,7	0,0	0,8	0,0	0,0	-1,0	-0,7	0,0	-0,8	-0,1	-0,5	0,0	0,2	0,0	-0,5	0,2	0,8	0,0	-0,6	-0,8	-1,0	-0,7	-0,7	-0,7	-0,8	-0,8	-0,7	-0,7	-0,8	-0,8	-0,7	-0,7	-0,8	-0,8	-0,8	-0,8	-0,7	-0,7	-0,8	-0,8
	ChIP-seq (peaks) ehmt2_P30_H3K27ac	0,0	0,7	0,0	-0,4	0,0	0,0	0,0	0,0	-1,2	0,0	0,0	0,0	-2,1	0,0	0,0	0,0	0,0	0,0	0,0	0,0	0,0	0,0	0,0	0,0	-1,9	0,0	-1,2	-1,0	0,0	-1,2	0,0	-0,3	0,0	-0,8	0,0	-0,8	-1,2	2,1	1,2	-0,3	1,4	1,0	0,8	0,0	0,0	1,1	-0,3	-1,3	0,0	0,0	0,0	0,0	0,7	-1,9	0,7	-1,2	0,0	-0,6	-0,6
	ChIP-seq (peaks) Ehmt2_P30_H3K4me3	0,0	0,0	0,0	0,0	0,0	0,3	-0,8	-0,8	-1,1	0,0	0,0	-1,7	-3,6	0,0	0,7	-4,8	-1,8	0,0	-0,7	0,0	-1,2	1,2	0,0	-0,3	-0,2	-2,6	-1,1	0,0	0,0	0,0	0,0	0,0	0,0	0,0	0,0	0,0	0,0	0,9	-0,1	-2,7	0,0	0,0	1,6	0,0	0,0	0,0	-1,4	-0,6	0,0	0,0	0,0	0,0	0,3	-0,1	-1,1	0,0	0,0	0,0	0,0
	ChIP-seq (prom) ehmt2_H3K4me1	-0,7	0,0	0,0	0,0	0,0	0,0	0,6	0,8	0,0	0,6	-0,6	0,0	-0,8	0,0	0,4	-1,9	0,6	0,0	0,0	-0,8	0,0	0,0	1,2	0,0	-0,3	0,0	0,0	-0,1	0,0	0,4	0,0	-0,1	0,0	0,5	0,0	0,2	0,0	0,3	0,0	-0,6	0,0	0,0	0,2	0,0	0,0	1,0	-0,4	0,3	0,0	0,0	0,4	0,0	0,0	0,0	0,0	0,0	0,0	0,0	2,1
	ChIP-seq (bodies) ehmt2_H3K36me3	0,0	0,0	0,0	0,0	0,0	0,0	0,0	-0,8	0,0	0,0	0,0	0,0	0,0	0,0	0,0	-0,4	0,0	0,0	0,0	0,0	0,0	0,0	0,0	0,4	-0,6	0,3	-1,2	0,0	0,0	-0,8	-0,8	-0,2	0,0	-0,8	0,0	0,0	0,0	-0,1	-0,2	-0,2	-0,9	-0,8	-0,8	-1,0	-1,0	-0,9	-1,0	-0,6	-1,0	-0,9	-0,8	-1,0	-0,9	-0,9	-0,7	-0,7	-0,5	-0,2	-0,3
	ChIP-seq (prom) ehmt2_H3K9me3	0,1	0,0	0,1	0,0	0,0	0,0	0,0	0,0	0,0	0,1	0,3	0,0	0,8	0,0	0,4	1,2	0,0	0,0	0,6	0,0	0,0	1,3	0,0	0,0	0,6	0,0	0,0	0,0	0,0	0,0	0,5	0,1	0,0	0,0	0,0	0,0	0,8	0,0	0,0	0,0	0,0	0,0	0,0	0,1	0,0	0,0	0,1	0,0	0,0	0,0	0,0	0,7	0,0	0,0	0,2	0,0	-0,2	0,0	0,0
	ChIP-seq (prom) ehmt2_H3K9me2	0,0	0,6	0,0	0,0	0,0	0,0	0,0	0,0	0,0	0,0	2,0	0,0	0,3	0,0	0,0	0,0	0,1	0,0	0,0	2,1	0,0	0,0	0,0	0,0	0,0	0,3	0,0	0,0	0,0	0,0	0,2	0,9	0,0	0,0	0,0	0,4	0,0	0,0	0,6	0,0	0,0	0,4	0,0	0,0	0,3	0,0	-0,2	0,0	-0,3	0,0	0,0	0,2	-0,5	0,0	0,0	0,8	0,0	-0,5	-1,1
	ChIP-seq (prom) ehmt2_H3K27me3	-0,4	-1,4	-0,8	0,0	-1,7	0,0	-1,9	-1,5	0,0	-0,8	-0,6	-0,8	0,0	0,0	0,0	0,0	-1,0	0,0	0,0	0,0	0,0	0,0	0,0	0,0	0,0	0,0	0,0	0,0	0,0	0,0	-0,4	0,0	0,0	-1,7	0,0	0,0	-0,6	0,0	0,0	0,5	0,0	0,0	0,0	0,0	0,0	0,0	-0,5	0,0	-0,6	0,8	-0,8	-0,7	0,0	-1,2	0,0	0,0	0,0	0,0	-0,8

DN-reg in *Ehmt1*$^{+/-}$ P30 only

DN-reg in *Ehmt1*$^{+/-}$ *and Ehmt2*$^{+/-}$ P30

ZSCORES

DN — UP

ZSCORE=-2.33 ZSCORE=0 ZSCORE=+2.33

B qPCR VALIDATION OF GRADIENT DOWN-REGULATION IN PCDHB CLUSTER

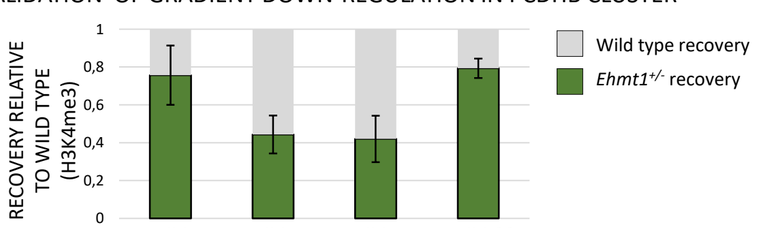

SUPPLEMENTARY FIGURE 7

A

		wt	*Ehmt1*$^{+/-}$	*Ehmt2*$^{+/-}$
Body weight (g)		25.05 ± 0.55	**23.23 ± 0.88 ***	25.90 ± 0.53
Rotarod- 4 to 40 rpm in 5 min (s)		155.25 ± 9.55	141.08 ± 15.28	141.38 ± 16.36
Grip strength (adjusted to body weight)		9.57 ± 0.29	9.16 ± 0.49	9.99 ± 0.42
Hot plate latency (s)		12.88 ± 1.29	14.75 ± 1.05	13.50 ± 1.27
Foot-shock sensitivity (mA)	***Flinch***	0.08 ± 0.00	0.08 ± 0.00	0.08 ± 0.00
	Vocalization	0.58 ± 0.09	0.64 ± 0.07	0.44 ± 0.08
	Jump	0.31 ± 0.04	0.34 ± 0.05	0.29 ± 0.04

B

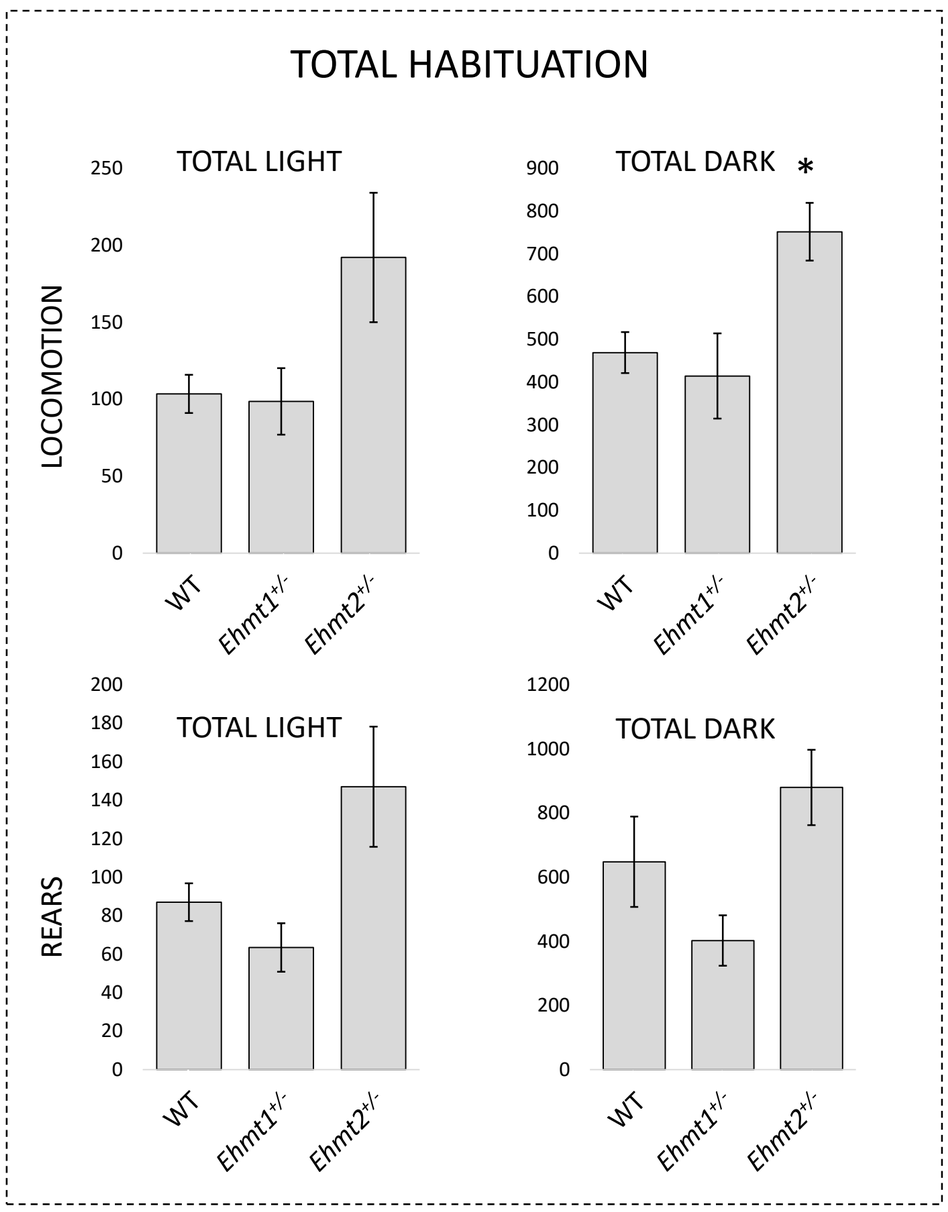

C

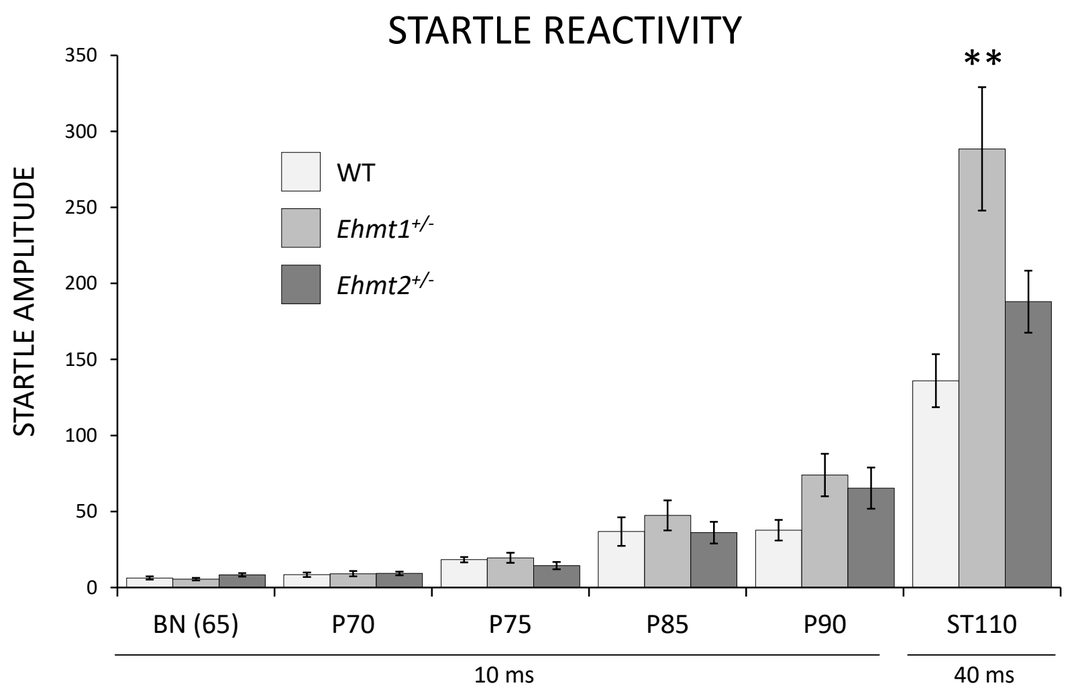

D

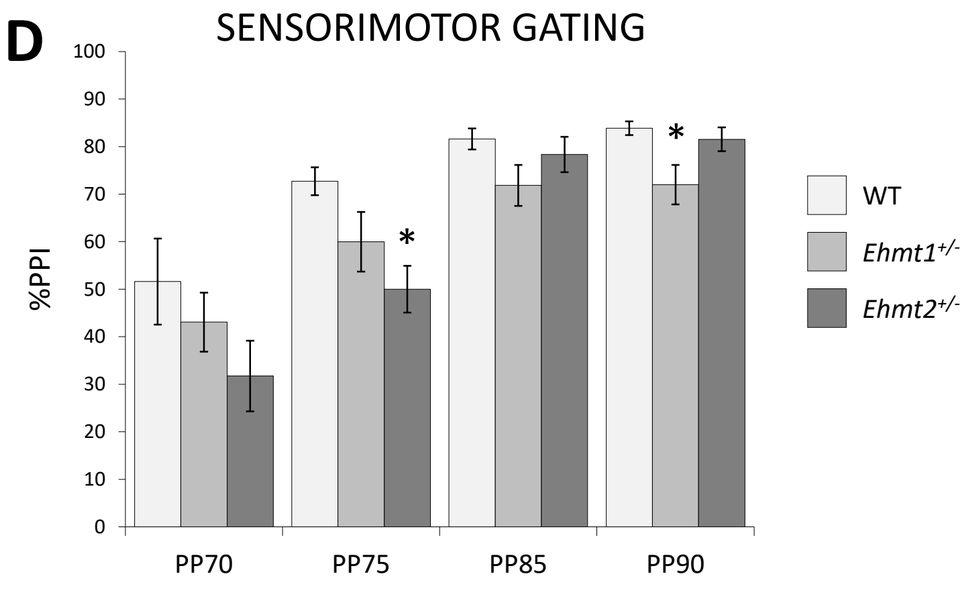

E

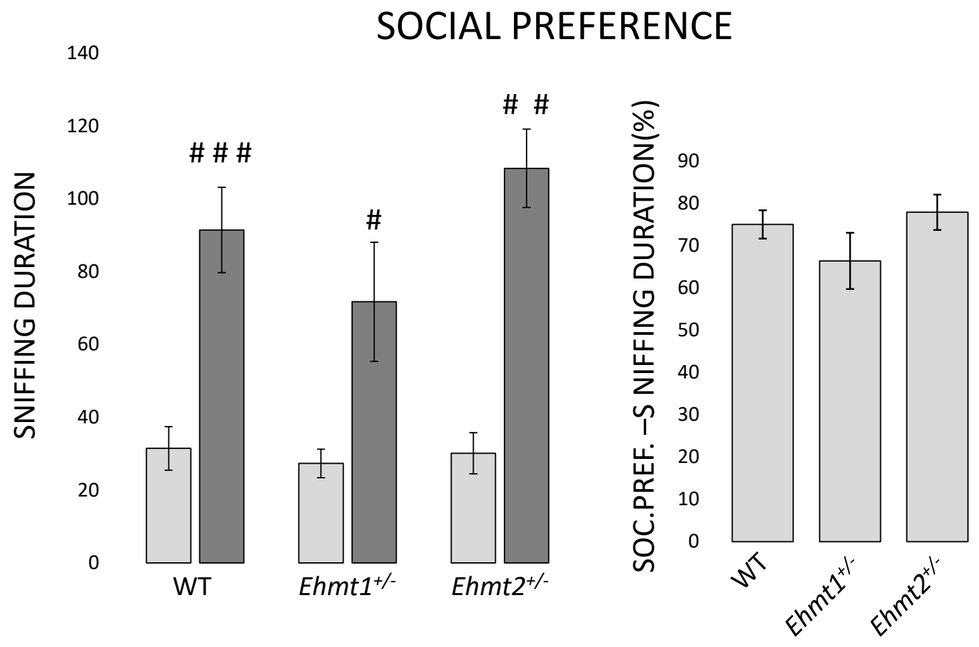

F

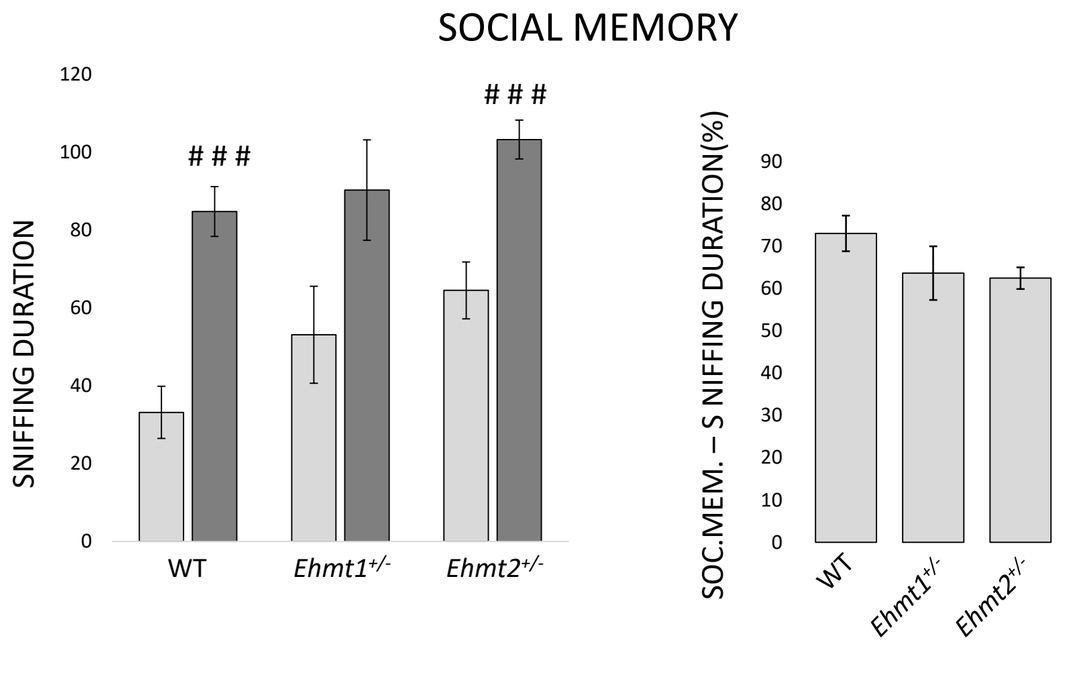

G

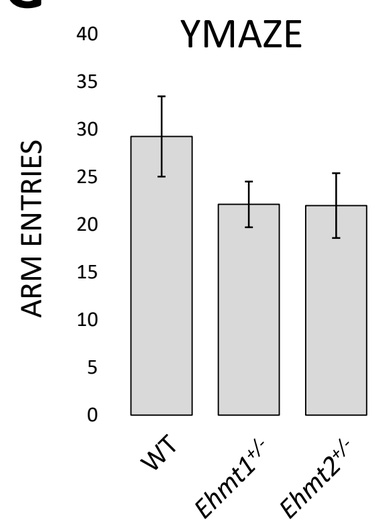

H

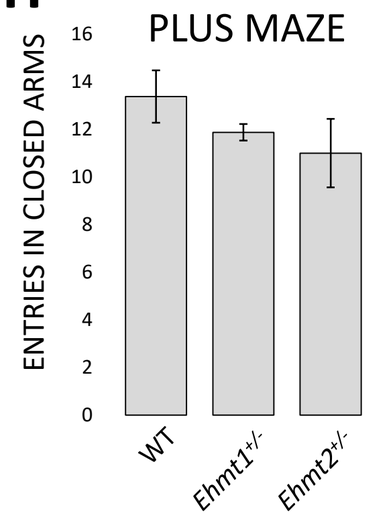

SUPPLEMENTARY FIGURE 8

A RNA EXPRESSION OF Ehmt2 (RNAseq)

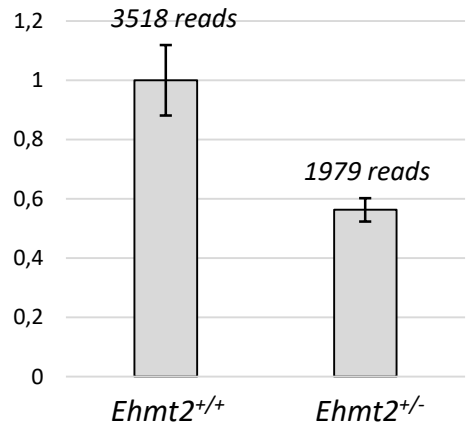

B WESTERN BLOT OF EHMT2